Inhibition Effect of Cysteine and Glycine towards the Corrosion of Cu10Ni Alloy in Sulfide Polluted Saltwater: Electrochemical and Impedance Study

Ahmed Abdel Nazeer [1,*], A.S. Fouda [2], E.A. Ashour [1]

[1] *National Research Centre, Electrochemistry and Corrosion Lab., Dokki, Cairo, Egypt.*
[2] *Department of Chemistry, Faculty of Science, El-Mansoura University, El-Mansoura-35516, Egypt.*

Received: 08 Jan 2011; Revised 17 Jan 2011; Accepted: 20 Jan 2011
[*] Corresponding author: E-mail: anazeer_nrc@yahoo.com

Abstract
Inhibition effect of cysteine (Cys) and glycine (Gly) towards the corrosion of Cu10Ni alloy in sulfide polluted NaCl solution was investigated using potentiodynamic polarization and electrochemical impedance spectroscopy (EIS) techniques. The results drawn from the two techniques are comparable. Addition of sulfide ions to NaCl solutions was found to accelerate the corrosion of the alloy. It was found that these investigated compounds act as good inhibitors for the corrosion of Cu10Ni alloy in polluted NaCl solutions. Potentiodynamic polarization curves revealed that both cysteine and glycine acted as mixed-type inhibitors. It was found that the adsorption of these compounds on Cu10Ni alloy surface follows Langmuir isotherm. EIS was used to investigate the mechanism of corrosion inhibition. The addition of KI was found to have a synergistic effect which enhanced the inhibition efficiency. The SEM results showed the formation of a protective film on the alloy surface in the presence of these additives.

Keywords: Corrosion, Cu10Ni alloy, NaCl, Na_2S, cysteine, glycine

1. Introduction

Copper base alloys have high corrosion resistance in various chloride media due to: i- in acidic medium, $E^{o}_{(Cu/Cu^{+})}$ is more positive than hydrogen evolution potential, therefore the spontaneous corrosion potential of Cu in the absence of the dissolved oxygen will be located at the immunity region [1] and ii- in neutral medium, a uniform and adherent film is usually formed at the metal surface, by corrosion products which act as a barrier layer against aggressive medium. Consequently, these materials are widely used in many industrial applications, such as, heat exchangers, electronic devices and fabrication of structures and components exposed to seawater and other marine environments [2, 3]. Cupronickels have good corrosion resistance to pitting attack [4-6]. The behavior of Cu10Ni alloy in NaCl has recently been the subject of extensive researches [7-10]. The corrosion behavior depends on the nature and characteristics of the passive film present on the alloy surface [11]. However, Cu10Ni alloy was found to suffer from corrosion when exposed to seawater polluted with S^{2-} ions [2, 12]. Syrett et al. [13] reported that the presence of S^{2-} ions is dangerous only when the corroding medium contains dissolved oxygen. Results showed that organic compounds containing nitrogen and their derivatives such as amines [14-22], amino acids [23, 24], containing sulfur [25, 26], and many others showed inhibition effect for the corrosion of Cu and Cu alloys in different media. Unfortunately, most of these compounds are synthetic chemicals which may be very expensive, toxic and hazardous to living creatures and environment e.g. benzotriazole (BTAH) [27] and its derivatives are excellent corrosion inhibitors for Cu and its alloys but these are toxic [28-30]. Recently, the research is oriented towards the development of green corrosion inhibitors [31]. Cysteine and glycine are chosen because: they are non-toxic, soluble in aqueous media and produced with high purity at low cost.

The aim of the present work is to investigate the effect of, eco-friendly inhibitors such as cysteine and glycine, on the corrosion behavior of Cu10Ni alloy in polluted 3.5% NaCl with sulfide ions solution. Also, the effect of addition of KI on the inhibition efficiency of these compounds is investigated.

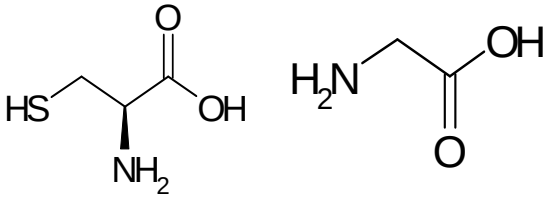

cysteine glycine

2. EXPERIMENTAL

2.1. Materials

Tests were performed on a commercial Cu10Ni alloy specimen of the following composition (weight %): 87.57 Cu, 10.68 Ni, 1.2 Fe and 0.55 Mn, which was provided from Abu-Qeer Power Station, Alexandria, Egypt. Na_2S was obtained from Ridel-de Haen while cysteine, glycine and NaCl were obtained from Aldrich chemical Co. Ltd.

2.2. Solutions

Solutions were prepared from AR grade chemicals and doubly distilled water. All measurements were performed in a solution containing 3.5 % NaCl which has a comparable salt level to that of seawater.

2.3. The electrochemical measurements

The potentiodynamic polarization measurements were performed using a Volta Lab PGZ 100 electrochemical system at E_{corr} after 30 min of immersion in solution. The measurements were carried out in a conventional three-electrode electrolytic cell. Saturated calomel electrode (SCE) and platinum foil electrode were used as reference and auxiliary electrodes respectively. The working electrode used for electrochemical measurements was in the form of a sheet (Cu10Ni) measuring 1x1 cm and fixed in polytetrafluoroethylene (PTFE) rods by epoxy resin in such a way that only one surface of area $1cm^2$ was left uncovered. The exposed surface was wet-polished with silicon carbide abrasive paper up to 1200 grit, washed thoroughly with doubly distilled water, degreased and dried with acetone. Polarization measurements were performed at potentials in the range from - 450 to -150 mV at a scan rate of $0.33mVs^{-1}$.

Electrochemical impedance spectroscopy (EIS) was carried out with a potentiostat/galvanostat (Gamry PCI 300/4) and a personal computer with EIS 300 software for calculations at E_{ocp} after 30 min. of immersion in solution. After the determination of steady-state current at a given potential, sine wave voltage (10 mV) peak to peak, at frequencies between $2x10^4$ Hz and 0.05 Hz were superimposed on the rest potential. The impedance diagrams are given in the Nyquist and Bode representation.

2.4.Scanning electron microscopy measurements (SEM)

The electrode surface of Cu10Ni was examined by Scanning Electron Microscope – type JOEL 840, Japan before and after immersion in polluted test solution in the absence and in presence of the optimum concentrations of the amino acids at 25°C, for 35 days immersion time. The specimens were washed gently with distilled water, then dried carefully and examined without any further treatments.

2.5. Quantum calculations

All the quantum chemical calculations were performed with Spartan student V4.1.0 semi-empirical program using PM3 method. The following quantum chemical indices were considered: the energy of the highest

occupied molecular orbital (E_{HOMO}), the energy of the lowest unoccupied molecular orbital (E_{LUMO}), ΔE = (E_{HOMO} - E_{LUMO}), dipole moment (μ), and Mulliken charges of cysteine and glycine.

3. RESULTS AND DISCUSSION

3.1. Open circuit potential measurements

Fig.1 represents the potential-time plots for Cu10Ni in 3.5%NaCl in the absence and in presence of different concentrations of S^{2-} ions.

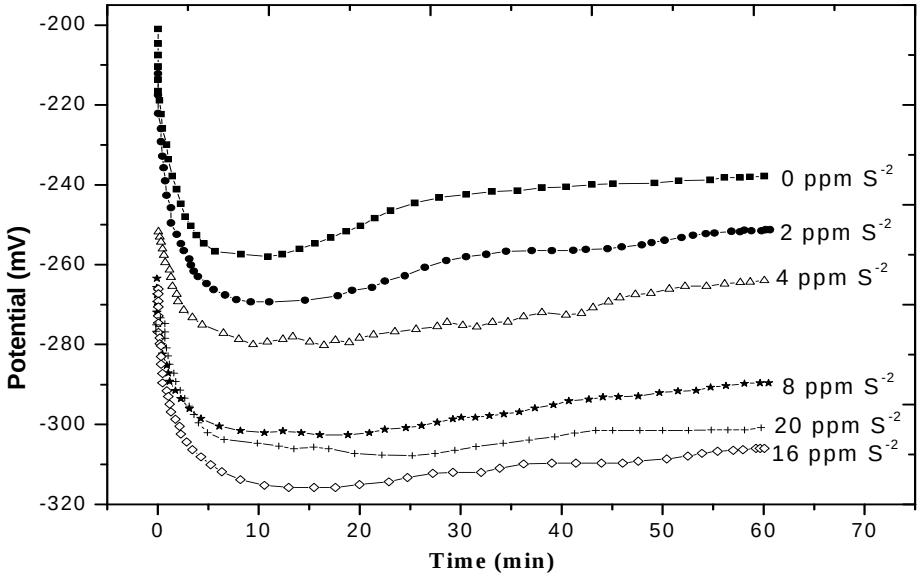

Figure 1. Potential-time plots for Cu10Ni in 3.5%NaCl in the absence and presence of different concentrations of sulfide ions.

The E_{OCP} curve in absence of S^{2-} ions is shifted from the first to more negative values (from -200 to -260mV). This behavior may be due to the dissolution of preliminary formed oxide film, which makes the anodic dissolution reaction faster [32]. After that, it is shifted to more negative direction for about 30 min before reaching a steady state potential (-240 mV). In the presence of S^{2-} ions, E_{corr} becomes more negative than in its absence, and increases by increasing sulfide ions and then decreases when S^{2-} concentration is 20ppm. This behavior may be explained on the basis that the anodic oxidation of S^{2-} ions is a complex process which might lead to the formation of polysulfide, elemental sulfur, thiosulfate, etc., according to the following reactions [33, 34]

$$3HS^- \rightarrow S_3^{2-} + 3H^+ + 4e^- \qquad E° = \ 0.097V \text{ (NHE)} \tag{1}$$

$$HS^- \rightarrow S + H^+ + 2e^- \quad E° = -\ 0.065V \text{ (NHE)} \tag{2}$$

$$2HS^- + 3H_2O \rightarrow S_2O_3^{2-} + 8H^+ + 8e^- \qquad E°=0.200V(NHE) \tag{3}$$

It was known that the formation of elemental sulfur on the electrode surface leads to its passivation. This can be used to explain the behavior observed at 20 ppm S^{2-} ions.

Fig. 2 shows the variation of the open circuit potential of Cu10Ni electrode with time in: a- 3.5 % NaCl + 16ppm S^{2-} (blank), b- blank + 100ppm cysteine and c- blank + 100ppm cysteine + 100ppm KI at 25 °C.

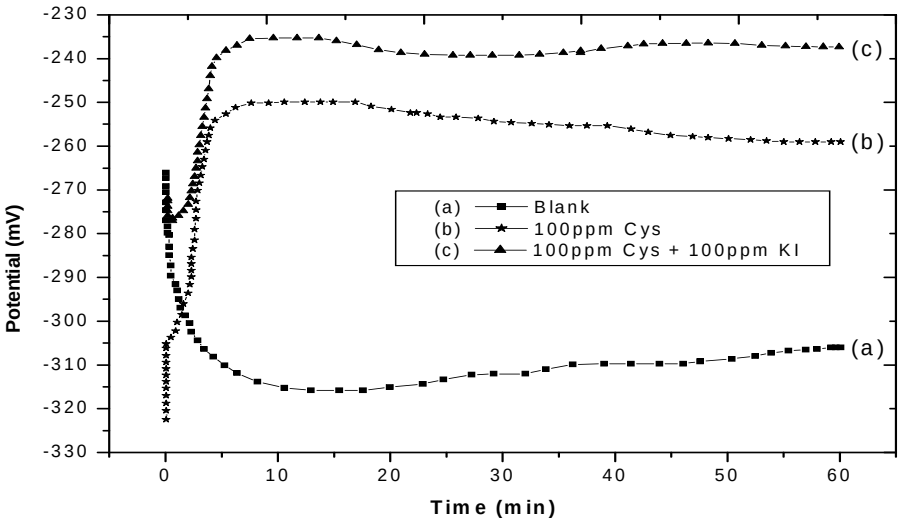

Figure 2. Potential-time plots for Cu10Ni in: a- 3.5%NaCl + 16ppm S^{2-} (blank) , b- blank + 100ppm cysteine and c- blank + 100ppm cysteine + 100ppm KI.

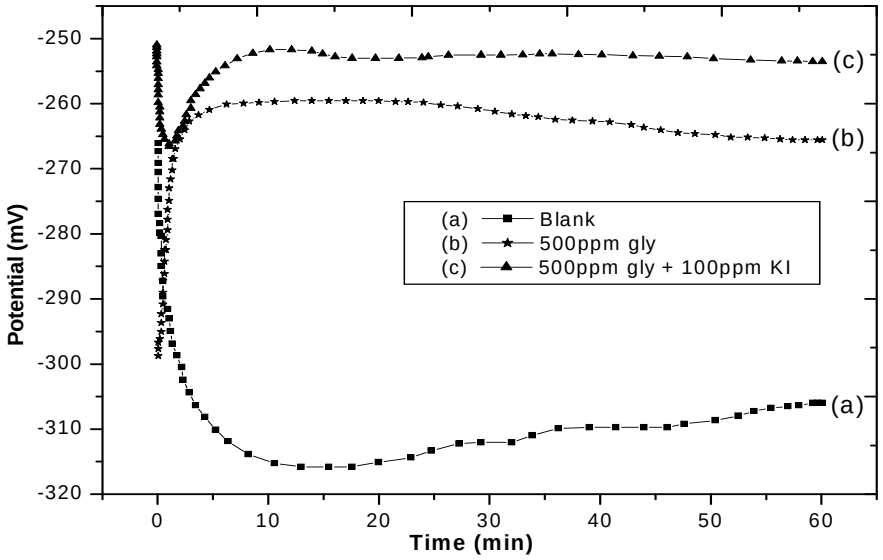

Figure 3. Potential-time plots for Cu10Ni in: a- 3.5%NaCl + 16ppm S^{2-} (blank), b- blank + 500ppm glycine and c- blank + 500ppm glycine + 100ppm KI.

Fig. 3 shows the variation of E_{ocp} of Cu10Ni with time in: a- blank, b- blank + 50ppm glycine and c- blank + 500ppm glycine + 100ppm KI at 25 °C.

Figs. 2b and 3b represent the variation of the E_{ocp} of Cu10Ni with time in polluted S^{2-} salt water in presence of cysteine (100ppm) and glycine (500ppm) at 25°C, respectively. Generally, the curves have almost similar features, where increasing the time of the test promotes the passivation of Cu10Ni electrode in this media and decreases the dissolution process. Within the experimental condition, this can be distinguished from the shift of the electrode potential towards more positive values with time. Generally, Cu10Ni is more prone to corrosion in solutions containing higher Cl^- and S^{2-} ions concentrations. In view of the value of pK_1 of H_2S ($pK_1 \approx 7$), one concludes that the predominant sulfide species in the polluted medium is HS^- [9]. The

presence of HS^- ions in the chloride medium increases the rate of the alloy dissolution and the formation of CuS, that is:

$$Cu: HS^-_{(ads)} = CuS_{(s)} + H^+ + 2e^- \quad (4)$$

In the presence of cysteine and glycine as inhibitors, the steady state potential is shifted in the positive direction. This indicates that the presence of cysteine and glycine species enhances the passivation process and retardation of the alloy dissolution, due to their adsorption on the alloy surface [35].

When the same experiments were carried out in sulfide polluted salt water in presence of 100 ppm cysteine or 500 ppm glycine with 100 ppm KI at 25°C, a significant change in potential was noticed (Figs. 2c and 3c). It seems that the optimum doses of the coupled additives are sufficient to form a protective and adherent film on Cu10Ni surfaces. This may be realized from significant shift in potential of Cu10Ni to more positive values than that recorded in the blank solution or in case of the single additives, in the absence of KI.

The obtained results may be explained in terms of a synergistic effect between the inhibitors with KI, since the positive potential shift in presence of the mixture is higher than that of the single ones. This can be attributed to the presence of KI facilitates the adsorption of cysteine and glycine on the alloy surface [20].

3.2. The potentiodynamic polarization curves

The potentiodynamic polarization curves of Cu10Ni alloy in 3.5 % NaCl solution containing different concentrations of S^{2-} were shown in Fig. 4. Addition of S^{2-} from 2 to 16ppm shifted E_{corr} to more negative values and when the concentration of S^{2-} ions at 20ppm, E_{corr} was shifted to more positive values. This is in a good agreement with the data obtained from the open circuit potential measurements.

Figs. 5 and 6 depicts the polarization curves for Cu10Ni alloy in sulfide polluted salt water free (curves 5a, 6a), containing 100ppm cysteine (curve 5b), containing 100ppm cysteine + 100ppm KI (curve 5c), containing 500ppm glycine (curve 6b) and containing 500ppm glycine + 100ppm KI (curve 6c), respectively.

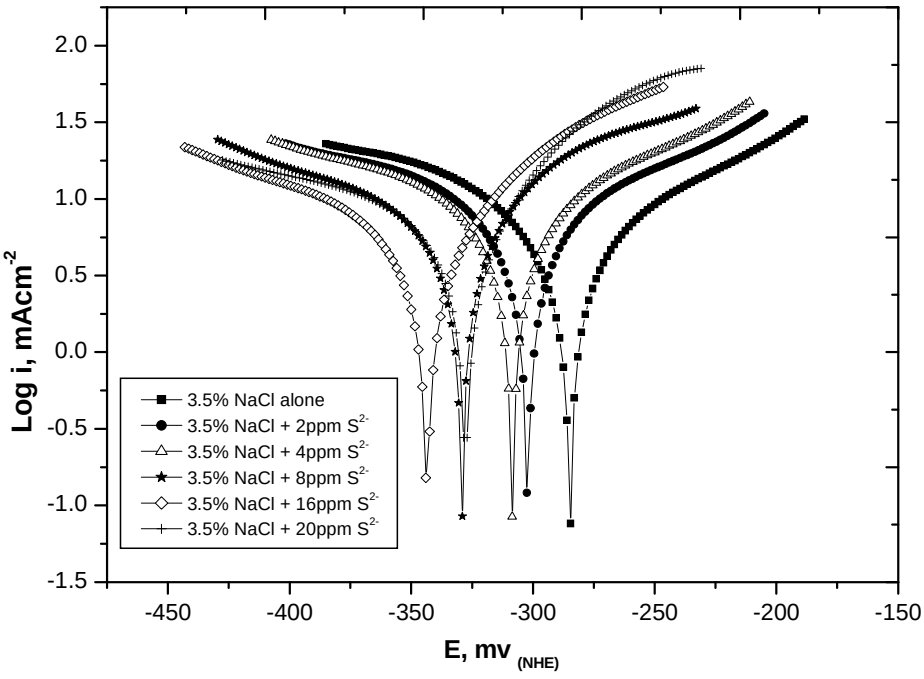

Figure 4. Polarization curves of Cu10Ni alloy in 3.5% NaCl at different concentrations of sulfide ions.

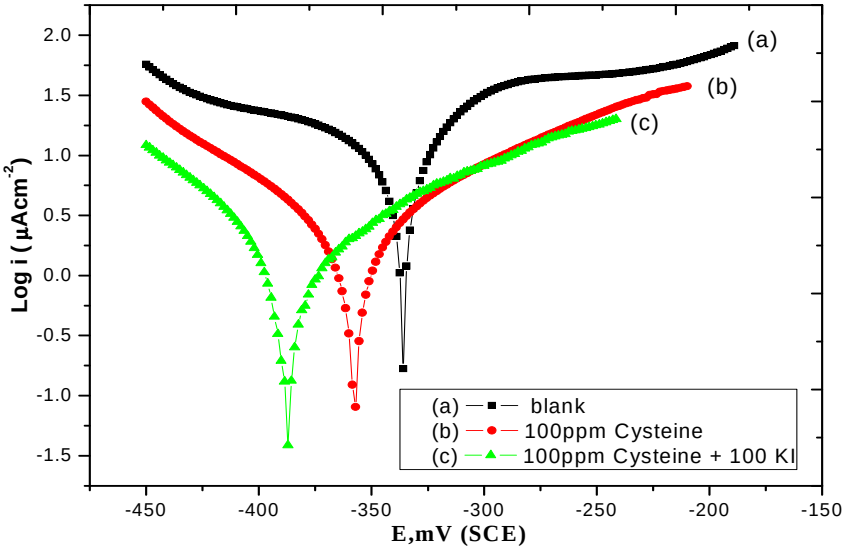

Figure 5. Polarization curve of Cu10Ni alloy in 3.5% NaCl+16ppm S^{2-} (a) with (b) 100ppm cysteine and (c) 100ppm cysteine + 100ppm KI.

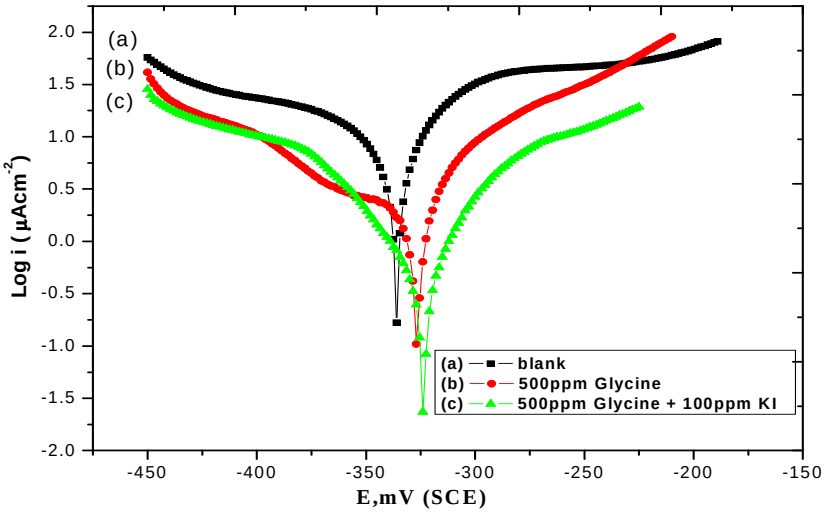

Figure 6. Polarization curve of Cu10Ni alloy in 3.5% NaCl+16ppm S^{2-} (a) with (b) 500ppm glycine and (c) 500ppm glycine + 100ppm KI.

When Cu10Ni electrode is immersed in sulfide polluted salt water, the potential marks a change with current density in both anodic and cathodic sides due to the effect of sulfide ions on the rate of alloy dissolution. The addition of KI to the test electrolyte produces pronounced effects compared to those observed in the presence of either cysteine, or glycine alone. It is clear from the curves of Figs. 5c and 6c that, the additives (cysteine + KI) shift $E_{corr.}$ of Cu10Ni electrode to the more negative values, while in case of the additives (glycine + KI) there is a slightly shift to less negative values. The Tafel slopes are constant indicating that there is no change in the mechanism of the process. The results show that these investigated compounds behave as mixed type inhibitors. The degree of surface coverage (θ) and IE% was calculated from the relations [24]:

$$\theta = [\, j_{corr,uninh.} - j_{corr,inh.} / j_{corr,uninh.} \,] \quad (5)$$

$$IE\ (\%) = [\ j_{corr,uninh.} - j_{corr,inh.} / j_{corr,uninh.}\ ] \times 100 \quad (6)$$

where $j_{corr,uninh}$ and $j_{corr,inh}$ are the corrosion currents in $\mu A\ cm^{-2}$ in the absence and presence of inhibitors, respectively. The kinetic corrosion parameters are listed in Table 1.

From the data depicted in Table 1, it has been found that the addition of KI to cysteine and glycine enhanced the corrosion inhibition efficiency of Cu10Ni alloy in such environments. The extent of corrosion inhibition depends on the surface conditions, the type and concentration of inhibitor, and the mode of adsorption of inhibitors [36]. The decrease in the R_p and increase in j_{corr} of Cu10Ni in additive-free sulfide polluted salt water solution can be ascribed to the dissolution of Cu due to the formation of $CuCl_2$ and Cu_2S.

In case of the addition of inhibitor, competitive surface adsorption between aggressive Cl^- and S^{2-} ions and the inhibitor molecules is assumed to occur [37, 38]. From the values of surface coverage, θ, it seems that a complete coverage of additives on Cu10Ni surface can occur and hence the severity of corrosion is decreased.

The results of these studies have shown that the inhibition of these investigated compounds (Table 1), suggests an appreciable contribution to the inhibition process via adsorption of cysteine, glycine and KI on the electrode surface [35, 36]. Moreover, this behavior may be ascribed to the ease of adsorption of cysteine and glycine in presence of KI.

Table 1. The effect of the optimum doses of inhibitors on the free corrosion potential (E_{corr}), corrosion current density (j_{corr}), Tafel slopes ($ß_a$ & $ß_c$), percentage inhibition efficiency (%IE), polarization resistance (R_p), corrosion rate (CR) and degree of surface coverage (θ) of Cu10Ni alloy in (3.5% NaCl + 16ppm S^{2-}).

Conc., ppm	$j_{corr.}$, $\mu A\ cm^{-2}$	$-E_{corr.}$, mV	$-\beta_c$, mV $dec.^{-1}$	β_a, mV $dec.^{-1}$	θ	%IE	R_p $\Omega\ cm^2$	corrosion rate (CR) mm/year
Blank	9.65	336	145	69	0.000	0.00	2.5	112.9
cysteine (100ppm)	1.08	357	73	75	0.888	88.8	9.8	19.9
cysteine (100ppm) + KI(100ppm)	0.52	387	66	68	0.946	94.6	13.4	10.5
glycine (500ppm)	1.80	327	94	30	0.813	81.3	6.2	25.3
glycine (500ppm) + KI (100ppm)	0.97	323	51	25	0.899	89.9	12.3	15.7

3.3. Adsorption isotherm

Adsorption isotherms are very important to determine the mechanism of organo-electrochemical reactions. It is important to know the mode of adsorption and the adsorption isotherm that fits the experimental results. In this part of the study, the obtained values of θ were fitted to different isotherms including Langmuir, Temkin, Frumkin, Dhar-Flory-Huggin, Friendlich, Parsons, Boockris-Swinkels and Henry isotherms. The best fit to the experimental data was obtained was obtained when Langmuir adsorption isotherm was used.

One of the forms of this isotherm is given by [39]:

$$C / \theta = C + 1 / K \quad (7)$$

$$\text{with } \Delta G^{o}_{ads} = - RT \ln (K_{ads} x 55.5) \quad (8)$$

where C is the bulk concentration of the inhibitor, K_{ads} the adsorption equilibrium constant and ΔG^{o}_{ads} the standard free energy of adsorption. Plot of C/ θ versus C was linear (Fig. 7) (correlation > 0.9), the deviation of the slope from unity (for ideal Langmuir isotherm) can be attributed to the molecular interaction among the adsorbed inhibitor species, a factor which was not taken into consideration during the derivation of Langmuir equation. Values of Langmuir adsorption parameters are recorded in Table 2. A value of - 40 kJ mol^{-1} is usually adopted as a threshold value between chemical and physical adsorption [40]. The higher values of K_{ads} suggested strong interaction of the inhibitors and the alloy surface [41]. The increasing of K_{ads} (Cys > Gly) reflects the increasing adsorption capability, due to structural formation on the metal surface [42].

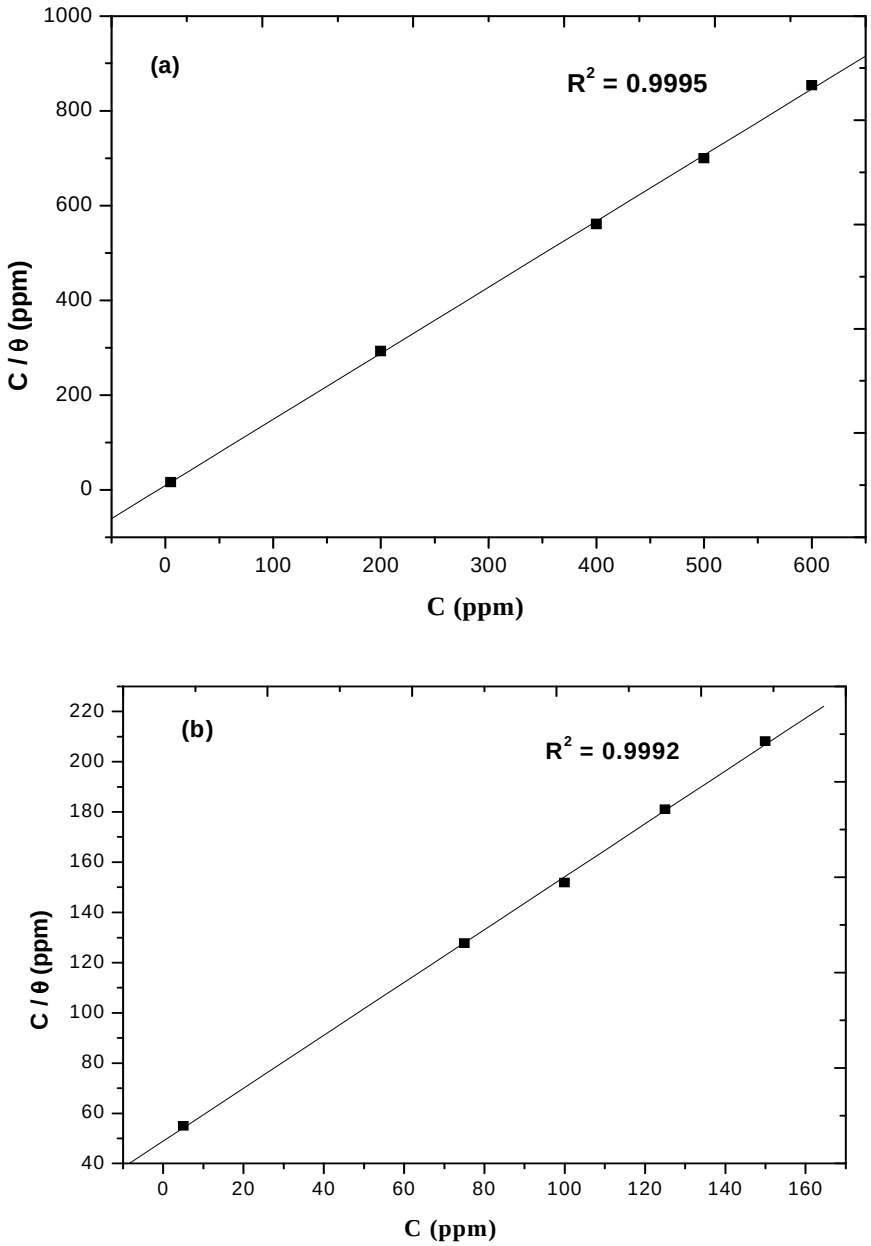

Figure 7. Langmuir adsorption isotherm of Cu10Ni alloy in 3.5% NaCl +16ppm S^{2-} containing different concentrations of (a) glycine and (b) cysteine.

Table 2. Adsorption coefficients deduced from Langmuir isotherm for glycine and cysteine.

Systems/ Concentration	Langmuir Isotherms			
	K_{ads} x 10^{-4} M^{-1}	Slope	R^2	$-\Delta G^{o}_{ads}$, kJ mol^{-1}
glycine	1.3	0.99	0.9995	33.4
cysteine	6.6	1.07	0.9992	38.5

3.4. Impedance Measurements

Electrochemical impedance is a powerful tool in the investigation of the corrosion and adsorption phenomena [43]. Figs. 8i and 9i show Nyquist plots of Cu10Ni alloy in sulfide polluted salt water in the absence and presence of inhibitors alone and with KI at 25^{o}C. The equivalent circuit model employed for this system is presented in Figure 10.

As shown in Figs. 8i and 9i each of them has an obvious capacitive loop in high frequency and a straight line (Warburg impedance) in low frequency. The capacitive loop is attributed to the relaxation time constant of the charge-transfer resistance (R_{ct}) whose value is approximately equal to the diameter of the capacitive loop and the double layer capacitance (C_{dl}) at the copper/electrolyte interface. The Warburg impedance reflects the anodic diffusion process of soluble copper species ($CuCl_2^-$) from the surface of the electrode to the bulk solution and the cathodic diffusion process of dissolved oxygen from bulk solution to the surface of the electrode.

The corrosion behavior of Cu10Ni alloy in the uninhibited solutions was influenced by mass transport. The impedance response of Cu10Ni alloy significantly changes in shape and size by addition of Gly and Cys alone and with KI. The presence of the inhibitors and KI in sulfide polluted salt water solutions change the mechanism of corrosion of Cu10Ni or at least may hinder the charge transfer from the Cu10Ni alloy surface.

R_s is the solution resistance, R_{ct} is the charge transfer resistance, W is the Warburg impedance and CPE is the constant phase element whose impedance is given by

$$Z_{CPE} = Y_o^{-1}(j\,\omega)\,n^{-1} \quad (9)$$

where Y_o is the constant phase element (CPE) of the electrical double layer, j is an imaginary number, $\omega = 2\pi f$ is the angular frequency (rad/s), *f* is the frequency of the applied signal, n is the CPE exponent for whole number of n = 1, 0, -1 CPE is reduced to the capacitor (C), resistance (R) and inductance (L) respectively. The value of n = 0.5 corresponds to Warburg impedance (W). The dispersion of the capacitive semicircle is related with surface heterogeneity due to surface roughness or inhibitor adsorption and formation of porous layer [44] and thus n serves as a measure of surface heterogeneity. Considering that the impedance of a double layer does not behave as an ideal capacitor, CPE is most often used to describe the frequency dependence of non ideal capacitive behaviour [45].

The inhibition efficiency (IE %) of the employed blends was calculated from the following equation:

$$IE\ (\%) = [(R_{ct} - R`_{ct}) / R_{ct}]\ X\ 100 \quad (10)$$

where R_{ct} and $R`_{ct}$ are the charge transfer resistance for the inhibited and uninhibited solutions, respectively.

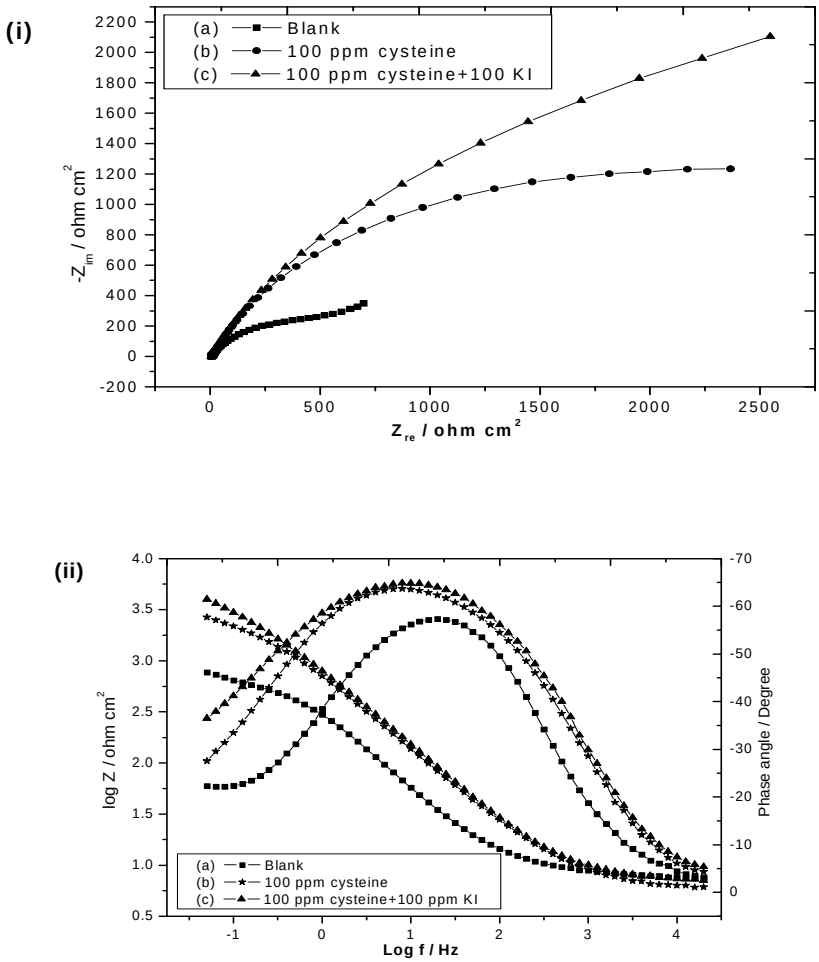

Figure 8. Electrochemical impedance spectra for Cu10Ni alloy in 3.5% NaCl + 16ppm S^{2-} solution containing 100ppm cysteine and (100ppm cysteine + 100ppm KI) at 25^0C i) The Nyquist plots ii) The Bode plots.

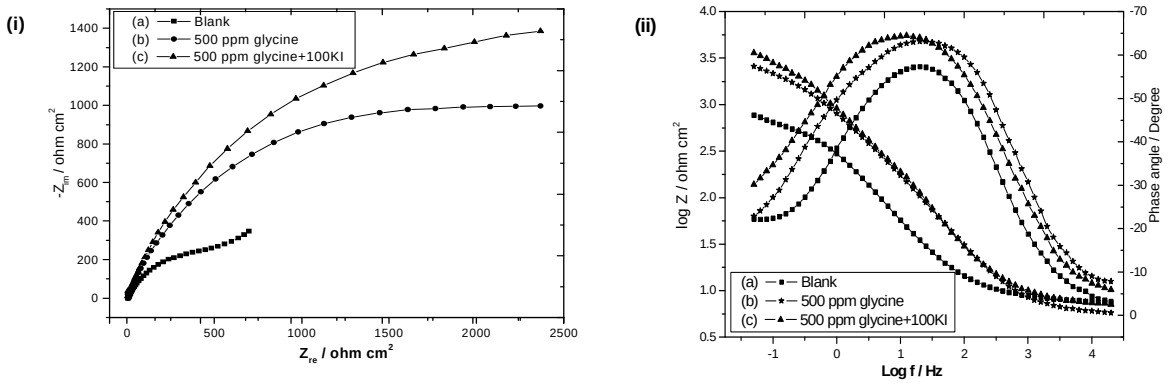

Figure 9. Electrochemical Impedance Spectra for Cu10Ni alloy in 3.5%NaCl + 16ppm S^{2-} solution containing 500ppm glycine and (500ppm glycine + 100ppm KI) at 25^0C i) The Nyquist plots ii) The Bode plots.

Table 3. Electrochemical kinetic parameters obtained by EIS technique for Cu10Ni in 3.5%NaCl + 16ppm S^{2-} (blank) solution containing optimum doses of glycine, cysteine and the coupled together glycine + KI and cysteine + KI at 25°C.

Conc., (M)	R_s (Ω cm^2)	R_{ct} (k Ω cm^2)	CPE		W Ω cm^{-2}	% IE
			Y_o (μF cm^{-2})	n		
Blank	6.267	0.573	574.6	0.72	0.0043	-
100ppm cysteine	6.580	2.686	122.4	0.70	0.0019	78.7
100ppm cysteine + 100ppm KI	7.133	4.207	83.9	0.76	0.0008	86.4
500ppm glycine	5.665	2.136	171.1	0.78	0.0017	73.2
500ppm glycine + 100ppm KI	6.004	3.063	107.8	0.74	0.0013	81.3

From the previous data (Table 3) we can conclude that the values of the CPE have decreased significantly in the presence of blends. The decrease in the CPE values may be due to the complex formation at the metal surface which reduces the thickness of the double layer. Therefore, the R_{ct} values have increased in the presence of blends indicating the corrosion inhibitive nature of blends [35]. The results of the impedance studies are in agreement with those obtained employing potentiodynamic measurements.

The Bode plots for Cu10Ni alloy after 30 min immersion in inhibitor free sulfide polluted salt water and blends are presented in Figs. 8ii and 9ii. The electrode impedance increases remarkably in the presence of the blends as compared to that in the single inhibitor indicating that the electrode surface becomes more passive. Also, the phase maximum at intermediate frequencies broadens in the presence of blends, which indicates the presence of a protective layer [46].

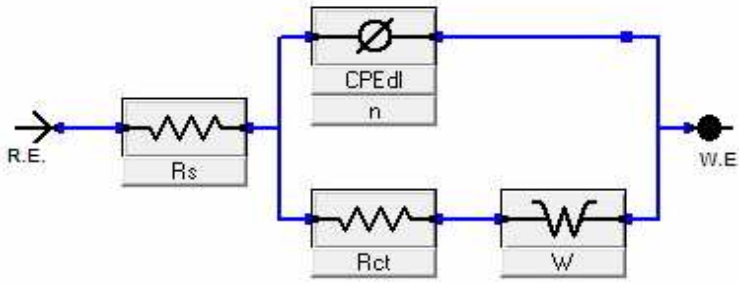

Figure 10. Equivalent circuit model used to fit the experimental EIS data.

3.5. SEM investigation

Fig. 11 (a-f) shows the scanning electron micrographs of Cu10Ni alloy surfaces before and after immersion in sulfide polluted salt water (3.5% NaCl + 16ppm S^{2-}) solution in the absence and presence of single additives (glycine and cysteine) and blends (500ppm glycine + 100ppm KI, 100ppm cysteine + 100ppm KI) used as corrosion inhibitors for 35 days.

Fig. 11 (a, b) displays SEM micrographs of clean and corroded alloy surface in polluted (3.5% NaCl + 16ppm S^{2-}), respectively. They clearly reveal the dangerous growth of localized corrosion with time of exposure in sulfide-polluted medium [9]. On the other hand, Fig. 11 (c-f) shows the micrographs of the alloy surfaces which were inhibited for 35 days in different media.

Immersion of the Cu10Ni samples in sulfide polluted salt water solutions containing the inhibitors glycine + KI (Fig.11, d) and cysteine + KI (Fig.11, f) shows that there is an improvement in the surface morphology compared to the corroded sample (Fig. 11, b). Also the adsorbed layers are more adhered and compacted than in case of glycine and cysteine alone (Fig. 11 (c, e)) respectively. This is due to the particles in case of (inhibitor + KI) are very fine than in case of glycine or cysteine alone which possibly diminishing the

corrosion areas due to covering the active sites. This process leads, in turn, to the coverage of the surface by a protecting film and hence a more homogenous surface is formed. This explains why the corrosion rate in the (inhibitor + KI) is lower than that measured in inhibitor-free solutions and in presence of glycine or cysteine alone.

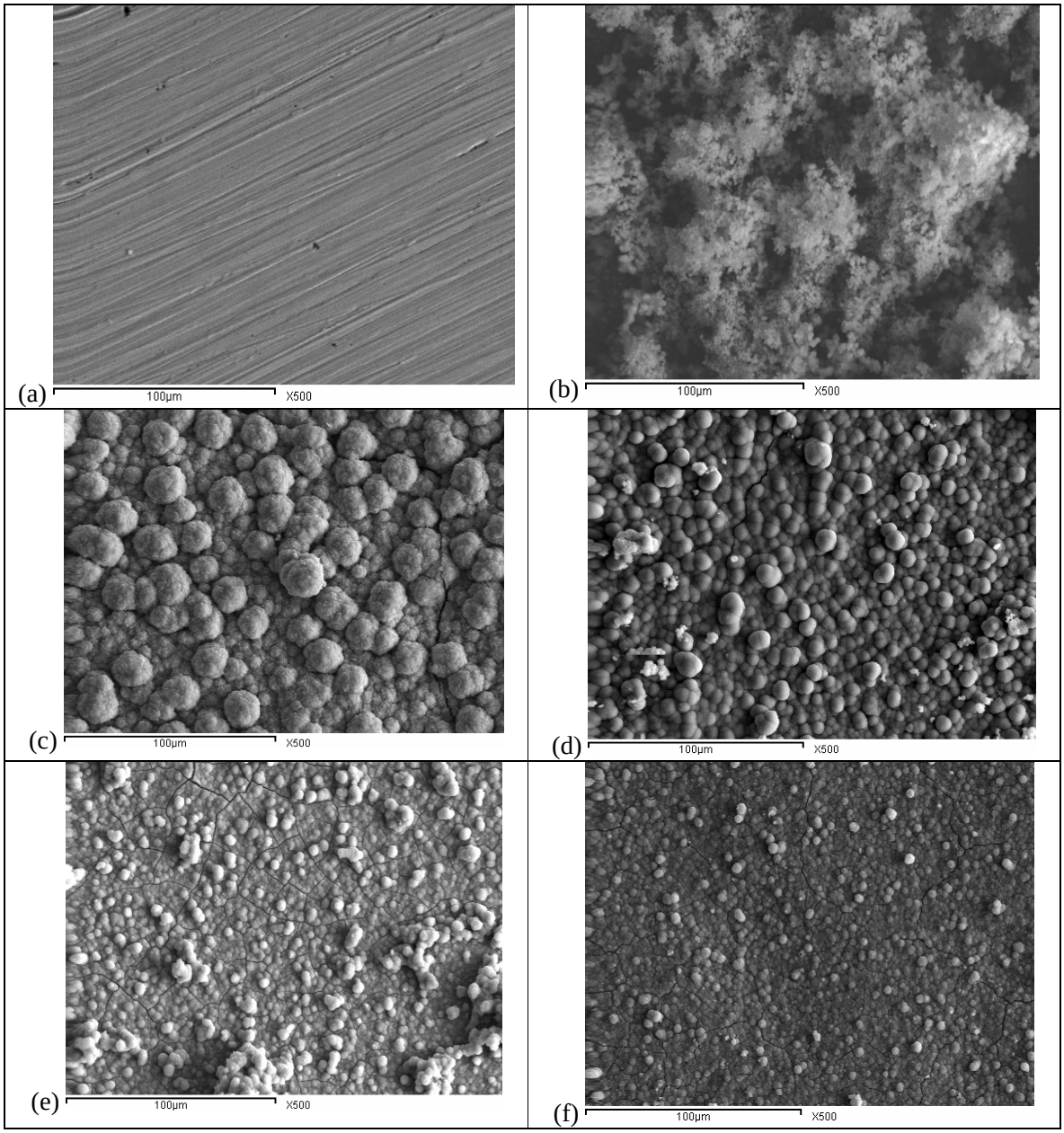

Figure 11. SEM micrographs of Cu10Ni alloy before and after immersion for 35 days in 3.5%NaCl + 16ppm S^{2-} solution with different concentrations of inhibitors (a) sample without immersion (clean sample), (b) in test solution, (c) test solution + 500ppm glycine, (d) test solution + 500ppm glycine + 100ppm KI, (e) test solution + 100ppm cysteine,(f) test solution + 100ppm cysteine + 100ppm KI.

3.6. Quantum chemical calculation using semiempirical method (PM3)

Semiempirical methods serve as efficient computational tools which can yield fast quantitative estimates for a number of properties [47]. Evaluation of the efficiency of cysteine and glycine as corrosion inhibitors for Cu10Ni alloy in sulfide polluted salt water have been performed using PM3 method.

Table 4. shows the quantum chemical calculation parameters (E_{HOMO}, E_{LUMO}, ΔE ($E_{HOMO} - E_{LUMO}$) and dipole moment (μ)) which have been calculated and correlated with experimental results. The optimized geometry of cysteine and glycine and their Mulliken charge densities are shown in Fig. 12.

Highest occupied molecular orbital energy (E_{HOMO}) and lowest unoccupied molecular orbital energy (E_{LUMO}) are very popular quantum chemical parameters. These orbitals, also called the frontier orbitals, determine the way the molecule interacts with other species. According to the frontier molecular orbital theory, the formation of a transition state is due to an interaction between the frontier orbitals (HOMO and LUMO) of reactants [48]. E_{HOMO} is often associated with the electron donating ability of the molecule. High E_{HOMO} values indicate that the molecule has a tendency to donate electrons to appropriate acceptor molecules with low energy empty molecular orbital. Increasing values of the E_{HOMO} facilitate adsorption (and therefore inhibition) by influencing the transport process through the adsorbed layer [49, 50]. E_{LUMO} indicates the ability of the molecules to accept electrons. The lower values of the E_{LUMO}, the more probable it is that the molecule would accept electrons. The HOMO-LUMO gap, i.e. the difference in energy between the HOMO and LUMO, is an important stability index. Low absolute values of the energy band gap (ΔE) gives good inhibition efficiencies, because the energy to remove an electron from the last occupied orbital will be low [51]. Similarly, low values of the dipole moment μ will favour the accumulation of inhibitor molecules on the metallic surface [52, 53]. From this table it is evident that, the energies of highest occupied molecular orbital (E_{HOMO}) decrease in the order: Cys > Gly. This in a good agreement with the previously mentioned experimental data obtained by potentiodynamic polarization and EIS techniques.

Table 4. Quantum chemical parameters for cysteine and glycine using semiempirical method

Calculated parameters	Cys	Gly
E_{HOMO} (eV)	- 9.50	- 9.87
E_{LUMO} (eV)	0.05	0.77
- ΔE (eV)	9.55	10.64
Dipole moment (μ) (Debye)	1.95	2.31
Molecular Weight (amu)	105.16	59.07

(a) (b)

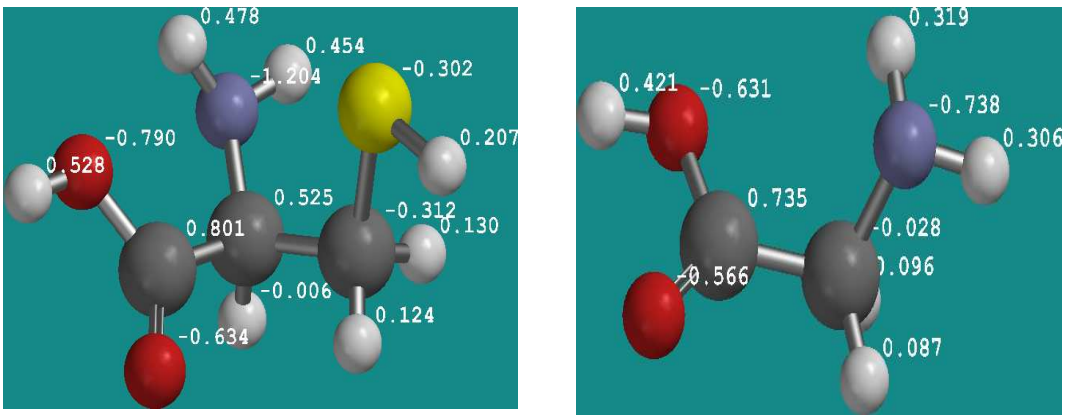

Figure 12. Optimized molecular structure of cysteine (a) and glycine (b) (ball and stick models) with their Mulliken population analysis.

3.7. Mechanism of inhibition

It is well-known that amino acids in acidic solutions are present in the cationic form, i.e.:

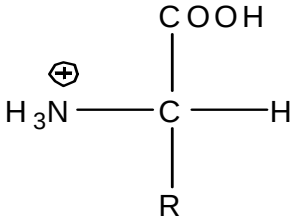

Depending on the charge of the metal or alloy surface one of the following adsorption processes will occur:

i) If the alloy surface is positively charged with respect to zero charge potential (PZC), Cl^- and HS^- first adsorb on the alloy surface, which in turn attract glycine and cysteine in their cationic forms and protonated water molecules. Therefore, a triple layer on the alloy surface will be formed and inhibit its dissolution.

ii) If the alloy or metal surface is negatively charged with respect to PZC, glycine and cysteine in their cationic forms and protonated water molecules will adsorb on the alloy surface directly.

iii) If the surface of the alloy or the metal attains no charge at PZC, neither the cationic nor the anionic forms adsorb on the alloy surface via ionic centers, but the adsorption may be due to the adsorption via the lone pair of electrons on the unprotonated N- atom and through the π–bond of the carbonyl group.

In our case, the investigated inhibitors should be in their cationic form and hence adsorption type (iii) will be the most suitable one.

4. Conclusion

The principle conclusions are:

1. Glycine and cysteine exhibited good inhibiting properties for Cu10Ni alloy corrosion in sulfide polluted salt water solution.
2. The Tafel plots of both glycine and cysteine indicated that these compounds act as mixed-type inhibitors.
3. Adsorption of these inhibitors at the Cu10Ni alloy surface in sulfide polluted salt water solutions are physical adsorption and give a good fit to Langmuir isotherm.
4. The presence of KI improves the inhibition efficiency, indicating that there is a synergistic effect between these amino acids and the iodide anion.
5. EIS results showed that the presence of cysteine and glycine in the test solution decreases CPE_{dl} and increases R_{ct}.
6. SEM examination of the alloy surface confirms the presence of a protective adsorbed film on the alloy surface.
7. From quantum chemical calculations, cys had the highest inhibition efficiency because it had the highest HOMO energy and lowest value of E_{HOMO} - E_{LUMO}.

References

1. Pourbaix, M. Atlas d'equilibre electrochimique, Gauthiers-Villard, 1963.
2. Eiselstein, L.E., Syrett, B.C., Wing, S.S., Caligiuri, R.D. *Corros. Sci.* 23(3) (1983) 223.
3. Reda, M.R., Alhaji, J.N. *Br. Corros. J.* 30 (1995) 1.
4. Wang, Y.Z., Beccaria, A.M., Poggi, G. *Corros. Sci*. 36 (1994) 1277.
5. Druska, P., Strehblow, H.H. *Corros. Sci*. 38 (1996) 1369.
6. Druska, P., Strehblow, H.H., Golledge, S. *Corros. Sci*. 38 (1996) 835.
7. Kear, G., Barker, B.D., Stokes, K.R., Walsh, F.C. *Electrochim. Acta*, 52 (2007) 1889.
8. Allam, N.K., Ashour, E.A., Hegazy, H.S., El-Anadouli, B.E., Ateya, B.G. *Corros. Sci*. 47 (2005) 2280.
9. Allam, N.K., Hegazy, H.S., Ashour, E.A. *Int. J. Electrochem. Sci*. 2 (2007) 549.
10. Allam, N.K., Ashour, E.A. *J. Appl. Surf. Sci*. 254 (2008) 5007.
11. Badawy, W.A., Ismail, K.M., Fathi, A.M. *Electrochim. Acta*, 50 (2005) 3603.
12. Richards, F. "*Chemical Oceanography" p.611, Academic Press*, New York. (1965).
13. Syrett, B.C., Macdonald, D.D, Wing, S.S. *Corrosion*, 35 (1979) 404.
14. Sherif, E.M., Park, S.M. *Electrochim. Acta*, 51 (2006) 4665.

15. Sherif, E.M., Park, S.M. *J. Electrochem. Soc*. 152 (2005) 428.
16. Stupnisek-Lisac, E., Brrnada, A., Mance, A.D. *Corros. Sci.* 42 (2000) 243.
17. Ma, H., Chen, S., Niu, L., Zhao, S., Li, S., Li, D. *J. Appl. Electrochem.* 32 (2002) 65.
18. Sayed, S.M., Ashour, E.A., Ateya, B.G. *Corros. Sci.* 36 (1994) 221.
19. El-Warraky, A.A. *Anti-Corros. Methods and Materials* 50 (2003) 40.
20. Ehteshamzadeh, M., Shahrabi, T., Hosseini, M.G. *J. Appl. Surf. Sci*. 252 (2006) 2949.
21. Singh, M.M. Upahyay R.B., Upahyay, B.N. *Bull. Electrochem.* 12 (1996) 26.
22. Al-Mobarak, N.A., Khaled, K.F., Elhabib, O.A., Abdel-Azim, K.M. *J. Mater. Environ. Sci.* 1 (1) (2010) 9.
23. Matos, J.B., Pereira, L.P., Agostinho, S.M.L., Baricia, O.E., Cordeiro, G.G.O., Elia, E.D. *J. Electroanal. Chem.* 570 (2004) 91.
24. Moretti, G., Guidi, F. *Corros. Sci*. 44 (2002) 1995.
25. Elmorsi, M.A. In Electrochem. Soc., Spring Meeting, Los Angelo's, CA, 96 (1996) 167.
26. Kumar, S., Narayanan, T.S, Kumar, M. S., Manimaran, A. *Int. J. Electrochem. Sci*. 1 (2006) 456.
27. Allam, N.K., Abdel Nazeer, A., Ashour, E.A. *J. Appl. Electrochem*. 39 (2009) 961.
28. Stupnisek-Lisac, E., Gazivoda, A., Modzarac, M. *Electrochim. Acta* 47 (2002) 4189.
29. Stupnisek-Lisac, E., Galic, N., Gasparac, R. *Corrosion* 56 (2000) 1105.
30. Varvara, S., Muresan, L.M., Rahmouni, K., Takenouti, H. *Corros. Sci*., 50 (2008) 2596.
31. Ismail, K.M. *Electrochim. Acta*, 52 (2007) 7811.
32. Rahmouni, K., Keddam, M., Srhiri, A., Takenouti, H. *Corros. Sci*. 47 (2005) 3249.
33. Valensi, G., Van Muylder, J., Pourbaix, M. in atlas of Electrochemical Equilibria in Aqueous Media, P. 545, M. Pourbaix, editor, NACE. Houston, TX (1974).
34. Ashour, E.A., Hegazy, H.S., Ateya, B.G. *J. Electrochem. Soc*. 147 (2000) 1767.
35. Badawy, W.A., Ismail, K.M., Fathi, A.M. *J. Appl. Electrochem*. 35 (2005) 879.
36. Badawy, W.A., Ismail, K.M., Fathi, A.M. *Electrochim. Acta*, 51 (2006) 4182.
37. Sobaramanyam, N.R., Mayanna, S.M. *J. Electrochem. Soc. India*, 33 (7) (1984).
38. Garrigues, L., Pebre, N., Dabosi, F. *Electrochim. Acta*, 41 (1996) 1209.
39. Damaskin, B.B., Petrii, O.A., Batrakov, V.V. Adsorption of Organic Compounds on Electrodes, Plenum Press, New York, 1971.
40. Hosseini, M., Mertens, S.F., Arshadi, M.R. *Corros. Sci*. 45 (2003) 1473.
41. Oguzie, E.E. *Corros. Sci*. 49 (2007) 1527.
42. Costa, S.L.F.A.DA, Agostinho, S.M.L. *Corrosion 45* (1989) 472.
43. Macdonald, J.R. Impedance Spectroscopy (New York, NY: John Wiley and Sons, 1987).
44. Popova, A., Christov, M. *Corros. Sci*. 48 (2006) 3208.
45. Hsu, C.H., Mansfeld, F. *Corrosion* 57 (2001) 747.
46. Badawy, W.A., El-Egamy, S.S., Ismail, Kh.M. *Brit. Corr. J*. 28 (1993) 133.
47. Gece, G. *Corros. Sci*. 50 (2008) 2981.
48. Fukui, K. Theory of Orientation and Stereoselection, Springer-Verlag, New York, 1975.
49. Ashassi-Sorkhabi, H., Shaabani, B., Seifzadeh, D. *Electrochim. Acta* 50 (2005) 3446.
50. Ozcan, M., Dehri, I., Erbil, M. *Appl. Surf. Sci.* 236 (2004) 155.
51. Moretti, G., Guidi, F., Grion, G. *Corros. Sci*. 46 (2004) 387.
52. Khalil, N. *Electrochim. Acta* 48 (2003) 2635.
53. Obot, I.B., Obi-Egbedi, N.O., Umoren, S.A. *Corros. Sci.* 51 (2009) 276.